Proceedings of the IASS 2024 Symposium
Redefining the Art of Structural Design
August 26-30, 2024, Zurich Switzerland
Philippe Block, Giulia Boller, Catherine DeWolf,
Jacqueline Pauli, Walter Kaufmann (eds.)

Experimental and numerical study on fire-induced pressure variation of the air-supported membrane structure

Yaning Zhang*, Ying Sun, Guoliang Wang, Yang Yu, Zhenggang Cao

*Key Lab of Structures Dynamic Behavior and Control of the Ministry of Education,
Harbin Institute of Technology, Harbin 150090, China
*Key Lab of Smart Prevention and Mitigation of Civil Engineering Disasters of the Ministry of Industry and Information Technology, Harbin Institute of Technology, Harbin 150090, China
School of Civil Engineering, Harbin Institute of Technology, 202 Haihe Road, Harbin, China.
1628736169@qq.com (Yaning Zhang)

Abstract

Air-supported membrane structures are sensitive to the pressure inside the structure, but there are few research on the change of internal pressure during fire. In this paper, based on the self-designed ignition and data measurement scheme, the fire test is carried out on the small size of 4 m x 2 m x 1 m air-supported membrane structure considering different fire source position, fire power, air leakage area and air supply. The time history of the temperature field and internal pressure inside the structure are obtained under the condition that the membrane surface is not damaged. Then a simulation study is conducted by the method of air leakage in subgrid in FDS software. The results show that the internal pressure rises rapidly to the maximum value gradually going down and then levels off after the ignition. This maximum value increases with the increase of air supply, fire power and the decrease of air leakage area and may be several times greater than the initial working pressure. The final stable internal pressure is slightly higher than the initial working pressure. The position of fire source has little effect on the internal pressure change after ignition. FDS software can well simulate the internal pressure variation of air-supported membrane structure after ignition.

Keywords: small size air-supported membrane structure, fire test, internal pressure variation

1. Introduction

An air-supported membrane structure is the construction that depends on internal pressurized air to form membrane surface tension and structural stiffness (Shen [1]), which has many advantages such as convenient construction, low cost and sustainability. In recent years, with the implementation of national fitness and environmental protection policies in China, air-supported membrane structures have been widely used in gymnasiums, coal sheds, etc. But they have also gradually exposed many problems in fire protection (Dong et al [2]).

Test and numerical simulation are two main research methods of the fire problem of air-supported membrane structure. Hopkinson, Custer, Thomas and Swedish laboratory [3-6] have all carried out fire tests, during which the development of the flame, the smoke, the membrane surface damage and structural collapse were recorded. Wang and Yi et al. [7-8] used FDS software to study the temperature field distribution characteristics and smoke flows. Wu, Cheng, Zhang et al. [9-11] also mainly investigated the temperature field under fire. In general, the fire resistance analysis of building structures is focused on the high temperature caused by fire. However, owing to their pressure-dependent properties for air-supported membrane structures (Feng et al [12]), internal pressure variation during fire should also be emphasized and it is necessary for thermal-mechanical coupling analysis (Zhang et al [13]). Yu et al. [14] took the lead in conducting some relevant research and

concluded that the air supply and air leakage area are important influencing factors. In fact, the fire-induced pressure has been more and more focused in the fire science research in recent decades, and it has been regarded as the potential risk of structural damage, mainly determined by the thermal shock of fire and the bearing capacity of the structure. Chow et al. [15] performed a simulation study on an indoor fire experiment reported in the literature by the Swedish Defense Research Agency and demonstrated that FDS can be applied in the study of indoor fire pressure changes. Janardhan, Hostikka, Brohez and Li et al. [16-20] also studied the pressure changes caused by indoor fires by means of experiments and simulations, and found that low leakage can prevent hot air from flowing out of the building, resulting in a rapid rise in air pressure within the structure, and if the pressure induced by fire is high enough, the door cannot be opened, which can seriously hinder evacuation and fire rescue operations. Together, the air tightness of buildings can bring new fire risks, and the air tightness of air-supported membrane structures is more stringent than that of traditional buildings, so the fire-induced pressure variation is worthy of in-depth study.

It is well known that simple fire simulation study differs greatly from reality and most fire tests of air-supported membrane structures have been carried out mainly at the end of the last century. Considering the characteristics of rapid conduction of pressure in space, the cost and feasibility of the fire test, etc., a small size air-supported membrane structure fire test is designed and carried out in present paper, and the internal pressure variation under different conditions is obtained. Then the simulation method by FDS software is validated against the test data.

2. Experimental study

2.1. Model design

A rectangular-planed air-supported membrane structures was designed to conduct the fire test using PVC-coated polyester fabric membrane with dimensions of 4m in length, 2m in width and 1m in height, an internal volume of about 3.23m³. The membranes were connected through thermal bonding process. The foundation adopted a steel frame which was compacted with counterweight concrete beams to avoid excessive internal pressure leading to the overall structural lifting. The corner position of the structure was arranged with a plurality of air nozzles for air supply or air leakage. In order to facilitate the collection of test data, a 12 cm diameter flange with small holes in the middle was assembled on the membrane surface through which the measuring equipment inside the structure connected to the outside. The front of the structure was equipped with an air-tight zipper for personnel to arrange the test conditions. Details of the test model are provided in Figure 1. Membrane materials relevant parameters are shown in Table 1.

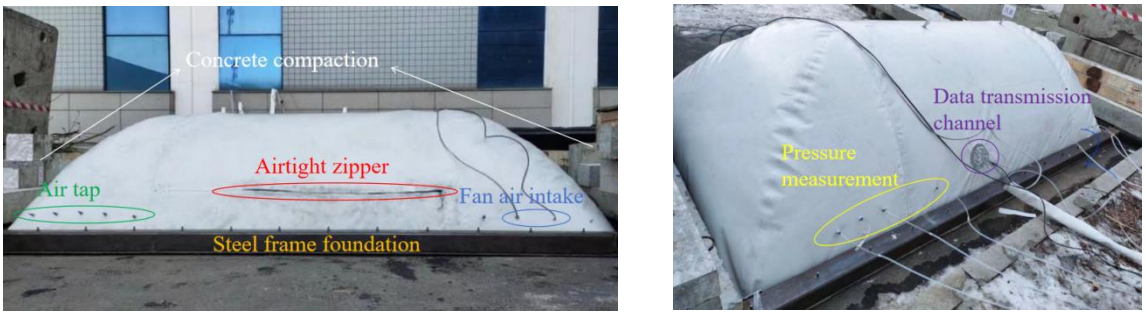

(a) Front view (b) Oblique view

Figure 1: Model design of small size air-supported membrane structure

Table 1: Membrane properties

Combustion performance	Density (kg/m^3)	Thickness (mm)	Conductivity (W/(m*K))	Specific heat (kJ/(kg*K))
B1	1350	1.1	0.07	1.17

2.2. Test scheme

The spaciousness of the internal space in the actual air-supported membrane structure usually

makes it challenging for the flame to contact and ignite the membrane surface in event of a fire. Therefore, the present test scheme is only for this case without considering membrane surface damage. Meanwhile, the experiment mimics the process from non-fire state to a fire state to get close to the real fire scene. To be specific, before the test, the structure was initially formed by blowing air from the zipper with a blower, and then the zipper was closed and the air pump was opened to inflate the structure sequentially. When there was obvious tension on the membrane surface, by adjusting the air supply and air leakage area, the internal pressure was stabilized near the normal working internal pressure. Finally the fire test was carried out. In addition, the hot air inside the structure was drained at the end of each operation, and then the tester adjusted and arranged the new operating condition. The test time is Harbin winter, the temperature is between -5°C±5.

2.1.1. Measurement

The air supply, fire power, internal pressure and temperature field were measured during the test. The temperature field results are mainly used to correct the fire simulation settings. Specifically, the air supply control and measurement equipment are shown in Figure 2. The maximum air supply of the air compression pump is 180 L/min. The pressure regulator is AR2000 and its range is 0.05Mpa ~ 0.8Mpa. The air flowmeter is MF5712, its measuring range is 0 L/min~200 L/min, and the accuracy is 0.01 L/min. The wireless pressure difference measuring instrument, model testo-510i, with a measuring range of 150hPa and an accuracy of 0.01hPa was adopted, as shown in Figure 3. A circular oil pan with airoline was used as the fire source and a 5cm thick water cushion layer was designed at the bottom in the oil pan to avoid airoline splashing caused by heat evaporation during airoline combustion. The fire power was measured by a high-precision electronic scale to record the time history curve of fuel mass loss, and the calculation formula is shown as Eq. (1), Where Q is the heat release rate (kW), α is the combustion efficiency of the fuel, $\dot{m}$ is the mass loss rate (kg/s), ΔH is the calorific value of airoline (MJ/kg). After much thought, the method of igniting fire source adopted remote control ignition device outside the structure, that is, electric sparks were generated remotely to ignite airoline. The details of fire source are shown in Figure 4. K-type thermocouples measured the temperature, and 9 thermocouples were fixed to 6 iron brackets and the coordinates of each temperature measuring point are shown in Figure 5.

(a) Air compression pump

(b) Pressure regulating valve

(c) Air flow meter

Figure 2: Air supply control and measuring equipment

Figure 3: Differential pressure

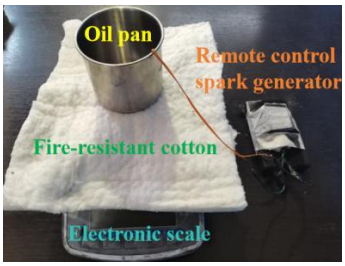

Figure 4: Fire source setup and measurement

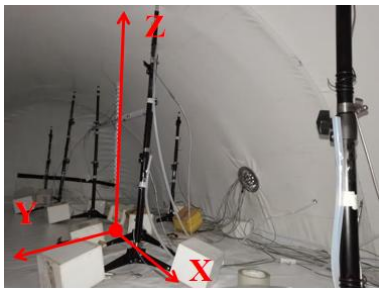

(a) Layout inside the structure

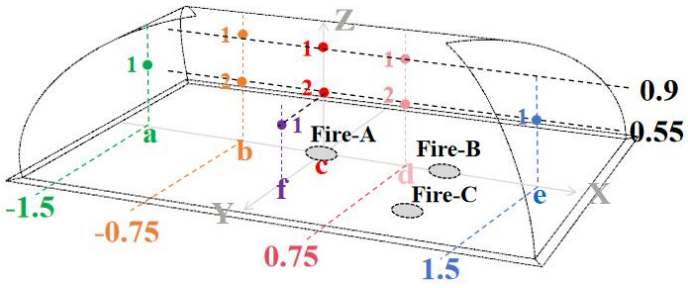

(b) Layout of the thermocouple tree and fire sources (m)

Figure 5: Arrangement inside the structure

$$Q = \alpha \times \dot{m} \times \Delta H \tag{1}$$

2.1.2. Operating conditions

The pressure control equipment in reality could adjust the internal pressure according to different weather, and usually increases the internal pressure to ensure the structural stability in the event of severe weather such as strong winds or heavy snow, but there may still be situations in which the equipment has no time to make adjustments. In view of this, 12 operating conditions (OC) were conducted and the details are indicated in Table 2.

Table 2: Parameter settings of test conditions

operating condition No.	Air Supply (L/min)	Inner diameter of the air nozzle (cm)	Diameter of the oil pan (cm)	Initial mass of the oil pan (g)	Location of the oil pan
1	60	1.0+0.4 (Two)	7	324.86	A
2	80	1.0+0.4 (Two)	7	328.42	A
3	100	1.0+0.4 (Two)	7	336.26	A
4	120	1.0+0.4 (Two)	7	330.83	A
5	100	0.8+0.4 (Two)	7	328.95	A
6	100	1.0	7	326.9	A
7	100	1.2	7	326.08	A
8	100	1.0+0.4 (Two)	5.5	268.37	A
9	100	1.0+0.4 (Two)	8	344.74	A
10	100	1.0+0.4 (Two)	11	351.81	A
11	100	1.0+0.4 (Two)	7	338.91	B
12	100	1.0+0.4 (Two)	7	305.81	C

Three Fire source positions (Fire-A、Fire-B、Fire-C) coordinates are respectively (0,0,0), (1.25, 0,0), and (1.25, 0.5, 0), as shown in Figure 5(b). During the test, the air leakage area of the structure can be adjusted by opening or closing the air nozzle of different sizes, and the fire power is controlled by different diameters of the oil pan. One point to be noted here is that the actual air-supported membrane structure is not completely sealed and with the increase of internal pressure, the inherent leakage area of the structure increases with the opening of small gaps, cracks and other leakage paths, and the actual leakage area caused by the air nozzle also needs to be adjusted due to the air shrinkage effect. The above corresponding equivalent air leakage area can be calculated by Eq. (2) in the subsequent analysis. Before fire test, the relationship between the equivalent air leakage area corresponding to the inherent air leakage of the small-size air-supported membrane structure is shown in Figure 6.

$$A_{\mathrm{eq}} = V_{\mathrm{in}} / \sqrt{2\Delta P / \rho} \tag{2}$$

Where A_{eq} is the equivalent air leakage area (m^2), V_{in} is the air supply (m^3/s), ΔP is the pressure difference (Pa), ρ is the air density (kg/m^3).

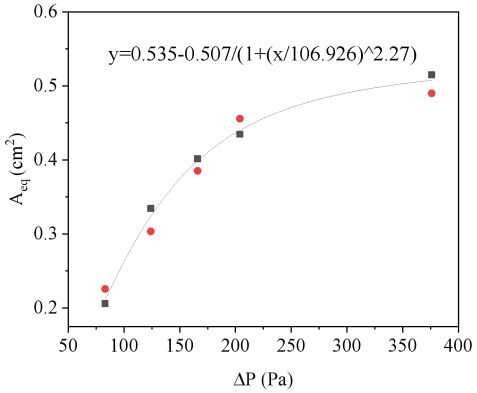

Figure 6: Relation between the equivalent air leakage area corresponding to the inherent air leakage and internal pressure of test model

2.3. Test results

2.3.1. Fire power

Figure 7(a) shows the recorded oil pan remaining mass change. The smoothed heat release rate curves under various operating conditions are shown in Figure 7(b) by Eq. (1). It can be found that the heat release rate curves of OC 1~7, 11 and 12 with the same oil pan size have almost a consistent performance, and their fire powers are approximately close. Meanwhile, the all heat release rates reached a maximum value immediately after ignition, and gradually decreased and finally tended to be stable. This was because the electric spark head placed at the airoline liquid level would burst and pop away when the remote ignition device was excited, and then the spilled airoline fell on the fireproof cotton under the oil pan and still kept burning. As a result, the combustion area of the oil pan was indirectly increased. In addition, the heat release rate of OC10 shows a trend of rising and gradually decreasing, and does not maintain a stable state, because less oil in test leads to a fuel quantity controlled combustion.

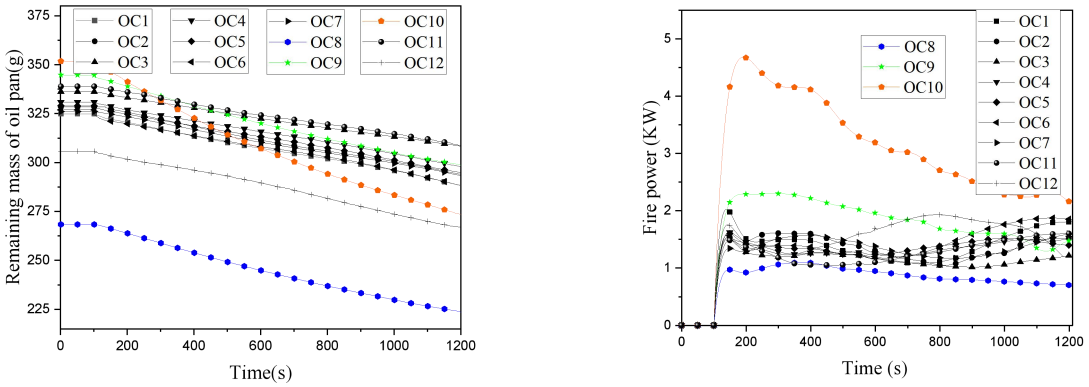

(a) oil pan mass change (b) heat release rate change

Figure 7: Results of heat release rate of fire

2.3.2. Temperature

As some thermocouples have no significant change, the results of only three thermocouples THCP-b-1, THCP-c-1 and THCP-d-1 close to the membrane surface are given, as shown in Figure 8. When the oil pan is 7cm, the maximum temperature of THCP-c-1 is between 30 °C and 40 °C. THCP-b-1 and THCP-d-1 were arranged symmetrically on both sides of the oil pan, and their temperature change is almost the same, and the maximum value is between 20 ° C and 25 ° C, indicating that the measurement of the thermocouple is reliable. When the size of the oil pan increases, the maximum temperature also increases. As a whole, the temperature field inside the structure presents an uneven distribution, where the air temperature near the membrane surface is higher than the lower air temperature except for the part of fire plume .

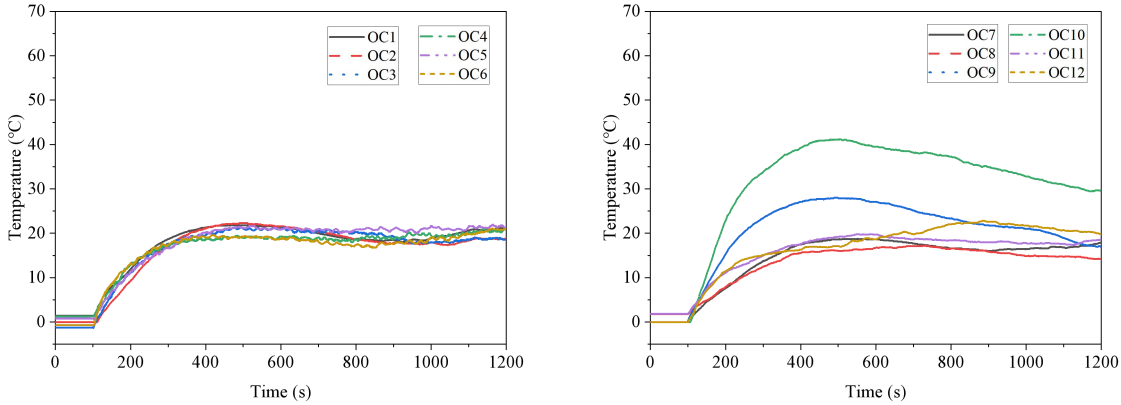

(a)THCP-b-1

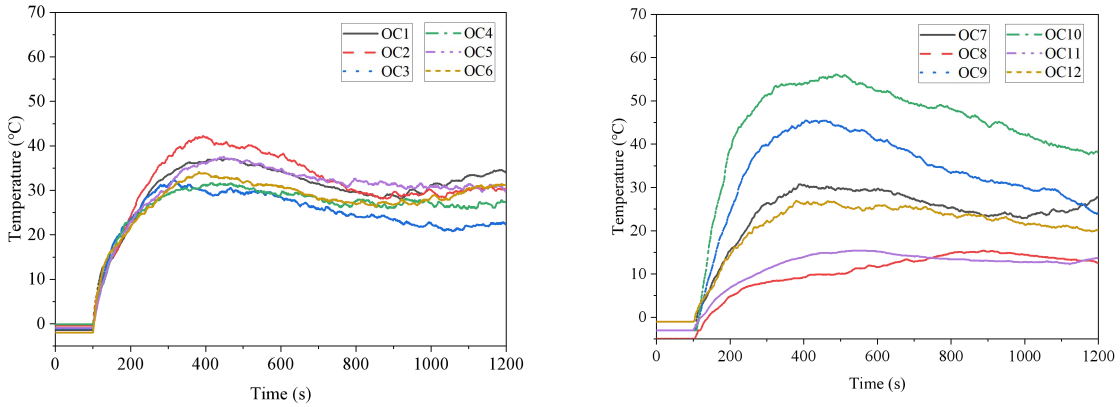

(b) THCP-c-1

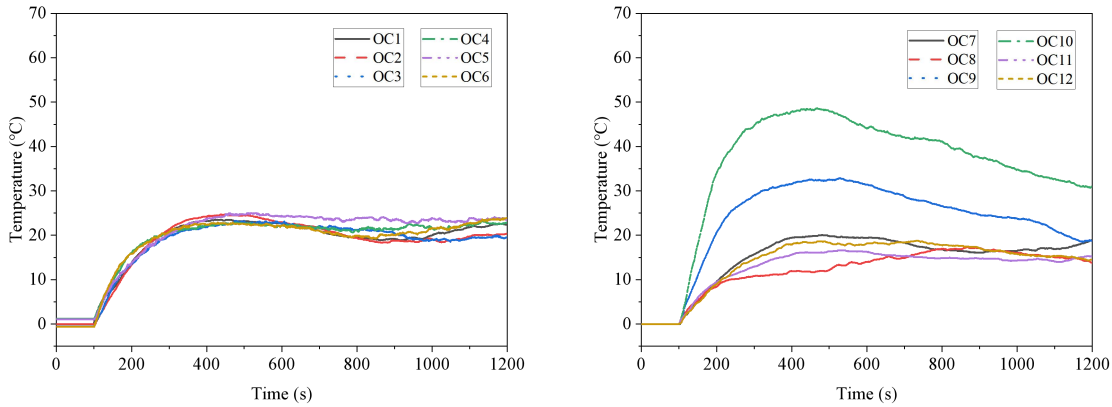

(c) THCP-d-1

Figure 8: Temperature results

2.3.3. Internal pressure

The internal pressure results are shown in Figure 9. The overall change trend of internal pressure is basically similar. Before ignition, the internal pressure is in a dynamic equilibrium state. After ignition, a lot of heat released by fire makes the air inside the structure expand. Due to the limited volume of the relatively closed space, its expansion effect is greater than the pressure loss effect caused by air leakage, so the internal pressure is in a rising state. With the increase of internal pressure, air leakage continues to increase. When the two effects are equal, the internal pressure reaches a peak value. Then, as the pressure loss effect is greater than the pressure boost effect caused by air expansion, the internal pressure gradually declines and finally reaches a relatively stable stage, where the internal pressure is larger than the stable internal pressure before ignition.

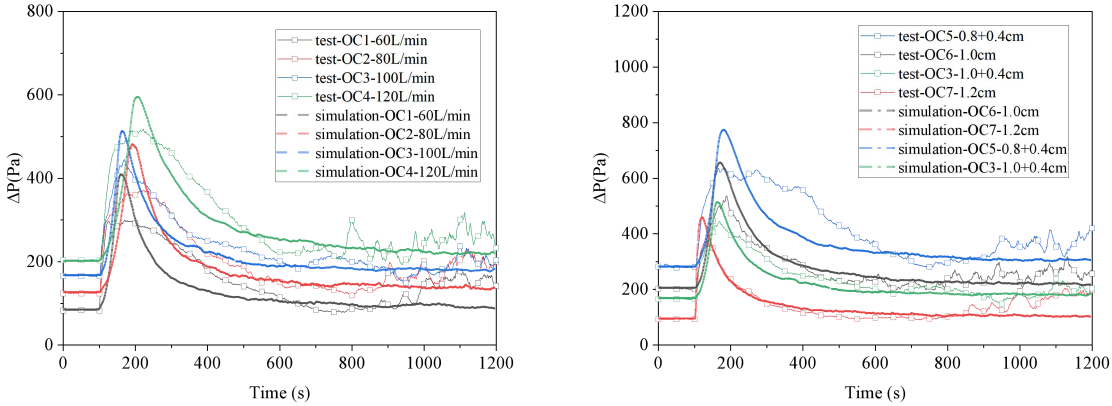

(a) different air supply (b) different leakage area

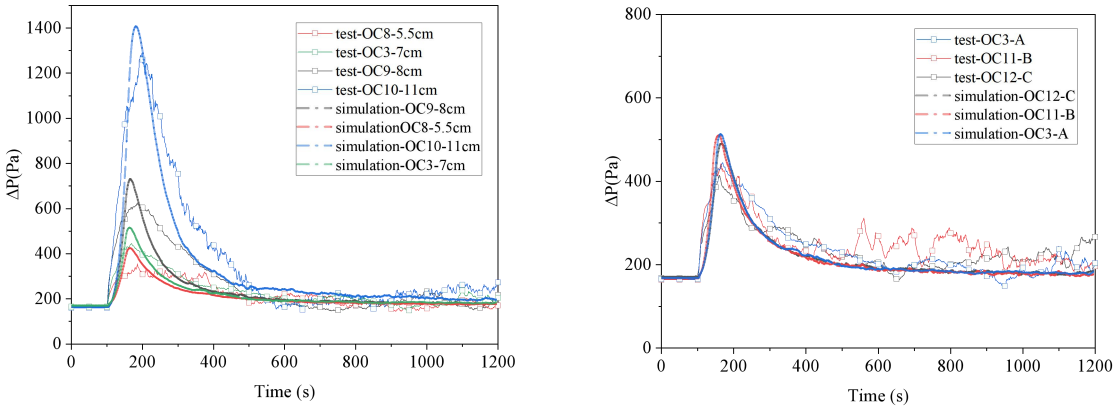

(c) Different fire power (d) different fire source location

Figure 9: Comparison of simulated and tests results of internal pressure variation

Figure 9(a) shows the influence of different air supply on internal pressure change. It can be found that with the increase of air supply, the stable pressure before ignition increases. This is because when the air supply increases in the same air leakage condition, a larger internal pressure can lead to a larger air leakage in order to make the air supply and air leakage equal. Meanwhile, the internal pressure reaches its peak value after ignition, and the peak internal pressure also increases with the increase of air supply. Figure 9(b) shows the influence of different air leakage areas on internal pressure change. It can be found that with the increase of leakage area, the stable pressure in the non-fire state decreases. This is because the increase of air leakage area leads to the increase of airleak volume. The peak internal pressure decreases with the increase of air leakage area. Figure 9(c) shows the influence of different fire power on internal pressure change. It can be found that the peak internal pressure increases with the increase of the size of the oil pan. Figure 9(d) shows the influence of different oil pan positions on the internal pressure change. Before ignition, the stable pressure is about 160Pa. After ignition, the peak value of internal pressure is approximately the same, and there is no significant difference. Considering the environmental impact and the possible errors of the equipment during all tests, it can be considered that the fire position has no significant influence on the internal pressure variation of the air-supported membrane structure.

3. FDS simulation study

3.1. Basic settings

The test structure's geometric model built by Rhino software was imported into FDS software to simulation study. A surface layer was set on the model surface and corresponding membrane material properties were assigned to this layer. In terms of air supply, the actual time history curve of air supply was set through "air support" in the "vent" module. In terms of fire source, four different heat release rates were simplified and specified as 1kW, 1.5kW, 2kW and 3kW after fitting the test data. The dimensionless expression D*/δx is used to calculate the appropriate mesh size, as shown in Eq. (3). The recommended ratio of D*/δx ranges from 4 to 16. In this paper, the mesh size of all operating conditions is uniformly 0.03m, and the mesh number is 420000.

$$D^* = \left(\frac{\dot{Q}}{\rho_\infty c_P T_\infty \sqrt{g}} \right)^{\frac{2}{5}} \tag{3}$$

Where $\dot{Q}$ is the heat release rate of the fire source (kW), ρ_∞ is the density of the ambient air (kg/m^3), c_P is the specific heat of the fluid (kJ/(kg·K)), T_∞ is the ambient air temperature (K).

3.2. Air leakage simulation method

The inherent air leakage is basically from the tiny holes. Although in some cases the leaking holes can be "concentrated" into a few grids, the leakage area rarely corresponds to the size of the grid cell, and the air flow rate through the holes may be very large, which can lead to the instability of the

numerical calculation in the simulation. The inherent air leakage of air-supported membrane structures is essentially a "subgrid" scale phenomenon, and it is unrealistic to define the leakage directly on the numerical grid of large eddy simulation solution.

In order to solve the above problem, "Zones" was used to designate the pressure zone of a closed room, and "leak area" was used to equivalent the air leakage area of a room to a "vent" connected to the external environment through a tiny pipe, and the air leakage was solved on a subgrid. In addition, FDS provides a "LEAK_PRESSURE_EXPONENT" parameter n, which can be used to simulate this relationship between the structure's inherent leakage and internal pressure, as shown in Eq. (4).

$$A_L = A_{L,ref}\left(\frac{\Delta P}{\Delta P_{ref}}\right)^{n-\frac{1}{2}} \tag{4}$$

Where $A_{L,ref}$ is the reference leakage area (m^2) at the reference pressure difference between adjacent areas. By default, n is 0.5, which means that the leakage area is pressure independent. In this simulation, n=0.64 was taken together with the data in Fig. 6. The value of leakage area of the air nozzle is determined by reference to Eq. (2) and Table 2.

3.3. Comparison of simulation results with tests

Fig. 9 also shows the comparison results of internal pressure variation of all operating conditions. The details can be seen in Table 3. It can be found that the difference between the test measuring value of the stable internal pressure before ignition and the simulated result is very small, indicating that the setting of the air supply and the air leakage conforms to the reality. Synchronously, the simulated peak internal pressure results are larger than the test results, in which the maximum error is 36.12% in OC1, and the average error of each operating condition is 19%. In addition, by sorting out the time to reach the peak internal pressure, it is found that most of the FDS simulation results are faster than the test measuring values, with a maximum error of 30 seconds and an average error time of 10 seconds. These are because the structure is rigid model not considering the change of structural shape in FDS. However, FDS can well simulate the internal pressure change trend of the structure under fire conditions on the whole.

Table 3: Comparison of FDS simulation peak internal pressure results with tests

OC	Test value (Pa)	Simulation value (Pa)	error(%)	Test time (s)	Simulation time (s)	error(s)
1	299	407	36.12	69	62	-7
2	370	480	29.73	122	97	-30
3	445	511	14.83	69	64	-5
4	516	593	14.92	122	107	-15
5	537	655	21.97	88	72	-16
6	374	455	21.66	29	22	-7
7	636	773	21.54	79	82	3
8	616	728	18.18	88	68	-20
9	355	421	18.59	86	66	-20
10	1287	1436	11.58	98	82	-16
11	414	489	18.12	61	66	5
12	429	508	18.41	64	60	-4

4. Conclusion and prospect

(1) Under the fire conditions without the membrane surface damage, the internal pressure has the similar development trend for air-supported membrane structures. After ignition, the pressure can rise to a peak, and then fall to a dynamic stabilization stage, at which the value of the internal pressure is slightly larger than the stable value before ignition. Before ignition, the stable pressure value increases with the increase of air supply and the decrease of leakage area. The peak pressure after ignition increases with increasing air supply, decreasing leakage area and increasing fire power. The position of the fire source has almost no effect on the development of internal pressure.

(2) The FDS software can well simulate the variation trend of the internal pressure during fire.

(3) Due to the characteristics of rapid conduction of pressure in space, the influence law of fire on internal pressure revealed in this paper is also applicable to full-size structures and can be used as a benchmark for the fire simulation of air-supported membrane structures.

Acknowledgements

The authors gratefully acknowledge the financial support of the National Natural Science Foundations of China (Project designation: 52178132 and Project designation: 52278167).

References

[1] S. Shen,"Membrane Structure: A new spatial Structure with Rapid Development," *Journal of Harbin University of Architecture and Architecture*, pp. 11-15, 1999.

[2] M. Dong, Y. Gu, L. Qiao, and Qu H.,"Review on Inflatable membrane structures," *Building Structures*, vol. 53, pp. 544-550, 2023.

[3] J. S Hopkinson, "Fire tests on an air supported structure," *Fire Safety Science*, vol. 955, pp. -1-1, 1972.

[4] R. L Custer,"Test burn and failure mode analysis of an air-supported structure," *Fire technology*, vol. 8, pp. 19-23, 1972.

[5] H. Thomas,"Pneumatic Structures, " *CrosbyLockwood Staples*, London, England, 1977.

[6] SP Swedish Nationgal Testing Institute,"Full scale fire test on composite membranes for textile structure," *SP Swedish National Testing Institute*, Boras, Sweden, 1998.

[7] Z. Wang,"Fire Resistance Analysis of rectangular Inflatable film Structures," *Master*: Xi 'an University of Architecture and Technology, Xian, China, 2014.

[8] Yi Celi and Zeng Bin,"Study on smoke movement characteristics of inflatable membrane structure under fire," *Fire Science and Technology*, vol. 35, pp. 476-480, 2016.

[9] J. Wu, G. Sun and S. Xue,"Numerical Simulation of Fire in Rectangular gas-borne Membrane Structures based on FLUENT," *in: The 17th Academic Conference on Spatial Structure*, Xi 'an, Shanxi, China, 2018.

[10] Z. Cheng, S. Xue and X. Li,"Progress and Prospect of research on fire resistance of coal shed with gas-supported membrane structure," *Building Structure*, vol. 51, pp. 583-587, 2021.

[11] H. Zhang,"Simulation of fire temperature field in large-space gas-bearing membrane structures," *Master*: Harbin Institute of Technology, Harbin, China, 2020.

[12] C. Feng, Z. Ni, K. Yang, X. Li, Y. Wang, and Y. Wang,"Analysis of measured displacement response of coal shed with gas-bearing membrane structure under adjusted internal pressure," *Building Structure*, 2022.

[13] Y. Zhang, Y. Sun, Q. Zhu, Z. Cao, and Y. Yu,"Thermal-mechanical coupling analysis of membrane surface failure of the air-supported membrane structure under fire considering weld seams," *Thin-Walled Structures*, vol. 198, 2024.

[14] Y. Yu, Z. Cao, Y. Sun, and Y. Wu,"Simulation of internal pressure FDS in gas-supported membrane structures under fire conditions," *Journal of Northeastern University (Natural Science Edition)*, vol. 43, pp. 1176-1182, 2022.

[15] W. K. Chow and G. W. Zou, "Numerical simulation of pressure changes in closed chamber fires," *Building and Environment*, vol. 44, pp. 1261-1275, 2009.

[16] R. K. Janardhan and S. Hostikka, "Experiments and Numerical Simulations of Pressure Effects in Apartment Fires," *Fire Technology*, vol. 53, pp. 1353-1377, 2017.

[17] S. Hostikka, R. K. Janardhan, U. Riaz, and T. Sikanen, "Fire-induced pressure and smoke spreading in mechanically ventilated buildings with air-tight envelopes," *Fire Safety Journal*, vol.

91, pp. 380-388, 2017.

[18]S. Brohez and I. Caravita, "Fire induced pressure in airthigh houses: Experiments and FDS validation," *Fire Safety Journal*, vol. 114, 2020.

[19]J. Li, T. Beji, S. Brohez, and B. Merci, "CFD study of fire-induced pressure variation in a mechanically-ventilated air-tight compartment," *Fire Safety Journal*, vol. 115, 2020.

[20]J. Li, T. Beji, S. Brohez, and B. Merci, "Experimental and numerical study of pool fire dynamics in an air-tight compartment focusing on pressure variation," *Fire Safety Journal*, vol. 120, 2021.